Biosensors and Bioelectronics 30 (2011) 324–327

Contents lists available at SciVerse ScienceDirect

Biosensors and Bioelectronics

journal homepage: www.elsevier.com/locate/bios

Short communication

Indication of intracellular physiological pH changes by L-cysteine-coated CdTe quantum dots with an acute alteration in emission color

Meifang Gui [a], Linjun Bao [a], Yunsheng Xia [a,*], Chao Wei [b], Shengzhou Zhang [b], Changqing Zhu [a,*]

[a] Anhui Key Laboratory of Chemo-Biosensing, College of Chemistry and Materials Science, Anhui Normal University, Wuhu, 241000, PR China
[b] Anhui Key Laboratory of Biotic Environment and Ecological safety, College of Life Science, Anhui Normal University, Wuhu, 241000, PR China

ARTICLE INFO

Article history:
Received 16 June 2011
Received in revised form 25 August 2011
Accepted 9 September 2011
Available online 16 September 2011

Keywords:
Physiological pH change
Cell image
Quantum dots
Emission color

ABSTRACT

A novel quantum dots (QDs) based biosensor was developed to monitor physiological pH changes in both fixed and living cells by means of pH-dependent emission color of the QDs. In our system, the nominally single-sized colloidal solution samples of the L-cysteine-capped CdTe QDs with intrinsically broadened size distributions were prepared by employing aqueous synthesis technique. The quench of fluorescence intensities of the QDs with a 16 nm red shift of the emission maximum and a color change from green to yellow was observed with a slight pH decrease (from 7.0 to 6.8) in the system. This pH-dependent emission could be attributed to the efficient exciton energy transfer from smaller QDs to larger ones, which was controlled by electrostatic-tuned aggregation/disaggregation (low/high pH values) processes of the QDs. In addition to high stability, the emission shift of the QDs was reversible for at least one cycle under optimal conditions. Our pH biosensor may find potential application for monitoring the intracellular pH changes in both physiological and pathological conditions.

1. Introduction

A large number of cellular processes are sensitive to intracellular pH (pH_i) (Jones et al., 1995). Typically, a dramatic transformation of the cell from a dormant to an active state has been found to be almost exclusively achieved by a pH_i change (Aronson and Boron, 1986). Clearly, pH_i change is important for a variety of cellular processes including cell proliferation and endocytosis (Helmlinger et al., 1997; Martin and Jain, 1994; Schindler et al., 1996), and also indicates some diseases (Ohmichi et al., 2005; Tang et al., 2007.). Intracellular alkalinization is an early event in the stimulation of mitogenesis in mammalian fibroblasts, where it may be necessary for the initiation of DNA synthesis (Moolenaar et al., 1984). Low pH also leads to various events such as hyperuricaemia, gout, and apoptosis (Matsuyama et al., 2000). Therefore, pH_i change is useful in understanding the regulation of cellular function and can be employed to screen some diseases at their early stage.

Among various methods currently available for the pH_i sensing, fluorescence technique is superior due to its high sensitivity and non-destructive nature (Tang et al., 2007). Up to now, majority of the sensing systems are based on the emission intensity changes. However, many factors might affect the emission intensity (Jr et al., 2002). Therefore, the development of simple probes that will give a measurable emission color change (Murphy, 2002) to visualize the pH_i change at a specific pH is highly desirable. Unfortunately, most of the current available probes often show only a single emission color that does not change substantially with pH (Ohmichi et al., 2005).

To obtain a measurable emission color change, a large emission shift is necessary. Meanwhile, the emission maximum of the probe must be located within a suitable wavelength range to satisfy the visible color change with a given emission shift. Currently, the design and development of the emission color-based sensing system remains a challenge. In terms of fluorescence probe, semiconductor nanoparticles or quantum dots (QDs) seem to be a desirable candidate since the intrinsic size-dependent luminescence properties of QDs (Alivisatos, 1996) allow us to choose a proper emission wavelength through tuning the particle size, which is different from conventional organic fluorescence dyes. On the other hand, the large emission shift often results from the reversible aggregation/disaggregation process of QDs (Moon et al., 2009; Narayanan and Pal, 2006), which can be performed by tuning non-covalent interaction between QDs, such as π–π and hydrogen bonding interactions (Liu et al., 2011).

Herein, we report a simple pH sensing system based on the aggregation/disaggregation process of QDs, which is governed by pH-tuned electrostatic interaction in single-sized L-cysteine (L-cys)-coated CdTe QDs samples. The acute alteration in emission color observed provides an intuitive indication for the physiological pH_i changes.

* Corresponding author.
E-mail addresses: xiayuns@mail.ahnu.edu.cn (Y. Xia), zhucq@mail.ahnu.edu.cn (C. Zhu).

0956-5663/$ – see front matter © 2011 Elsevier B.V. All rights reserved.
doi:10.1016/j.bios.2011.09.005

2. Experimental

2.1. Materials

L-cys and Te powder (60 mesh, 99.999%) were purchased from Alfa Aesar. $NaBH_4$, $CdCl_2{\cdot}2.5H_2O$, HCl, NaOH and other routine chemicals were acquired from Shanghai Reagent Co. All solutions were prepared with double deionized water.

2.2. Instruments

A Hitachi-U-3010 spectrometer was used to record the UV-visible spectra. Steady-state fluorescence measurements were performed using a Hitachi F-4500 spectrofluorometer equipped with a R3896 red-sensitive multiplier and a 1 cm quartz cuvette. Fluorescence lifetime measurements were performed with the time correlated single photo counting technique on the combined steady state and lifetime spectrometer (Edinburgh Analytical Instruments, FLS920). Characterizations of transmission electron microscopy (TEM) were carried out on Tecnai G2 20 ST (FEI) under the accelerating voltage of 200 kV. The samples for TEM measurements were prepared by the deposition of one drop of aqueous dispersion on a copper grid coated with thin films of carbon, and the solvent was removed by evaporation in air. The pH values were measured with a model PHS-3C pH meter.

2.3. Preparation and purification of L-cys-coated CdTe QDs

CdTe QDs capped by L-cys were directly synthesized in water and purified according to the modified literature procedure (Gao et al., 1998). A mass of 0.2864 g (1.25 mmol) of $CdCl_2{\cdot}2.5H_2O$ was dissolved in 100 mL of double-distilled water, and 3.0 mmol of L-cys was added under stirring, followed by pH adjustment to 11.2 by dropwise addition of 1 M NaOH solution. The solution was deoxygenated by bubbling N_2 through the solution for 40 min. Freshly prepared, oxygen-free NaHTe was then injected into the above solution with stirring. The molar ratio of Cd^{2+}/cys/HTe^- was 1:2.4:0.5. The resulting mixture was heated at 100–120 °C and refluxed for different amounts of time to grow the particles to the desired size. For the L-cys-coated CdTe QDs with the mean diameter of 2.6 nm (QDs-1), the reflux time of 50 min was used.

To purify QDs-1, the crude solution of the nanoparticles was dialyzed against NaOH aqueous solution at pH 11.0 to remove excess precursor reagents with the dialysis membrane. The concentration of the crude colloidal solution of QDs-1 was estimated to be 6.0 mM according to the final concentration of NaHTe. The dialyzed solution was diluted to 0.3 mM as a working solution for further experiments.

2.4. Gel electrophoresis

Gel electrophoresis (BioRad, Hercules, CA) was employed to investigate the effect of pH on the electrophoretic mobility of L-cys-coated QDs. Lambda DNA/Hind III markers were used as references. Agarose gels (1%) containing ethidium bromide were cast in neutral pH buffer (pH 7.0, 10 mM MES) and in weak acid pH buffer (pH 6.8, 10 mM MES). 0.1 M NaOH was used to adjust the pH of the buffers. QDs solutions were separated on the 1% agarose gel, visualized, and photographed under UV light.

2.5. QDs uptake by HepG2 human liver cancer cells

Human hepatocellular carcinoma cell lines (HepG2 cells, Manassas, VA) were maintained in DMEM (Life Technologies, Inc., Invitrogen, Carlsbad, CA) plus 10% heat-inactivated fetal bovine serum at 37 °C in a humidified incubator with 5% CO_2. Cells were subcultured for 24 h before experiments to produce a concentration just below confluence. A volume of 50 μL of the QDs was added to the DMEM over the cells and was incubated for 1 h at 37 °C. Before performing fluorescence observations, cells were washed with PBS three times. For cell fixation, HepG2 cells (grown in coverglass chambers) were rinsed three times with PBS, immersed in 4% formaldehyde buffer (37% formaldehyde diluted with PBS) at room temperature for 20 min, and finally washed three times with PBS. Fixed cells were dried gently with compressed air.

3. Results and discussion

3.1. Characterizations of QDs-1

Compared with the synthesis of QDs in organic medium, aqueous synthesis provided high water-solubility (Xia and Zhu, 2008), but often suffered from broad fluorescence. In our case, however, L-cys-coated CdTe QDs synthesized following the latter strategy were demonstrated to be a suitable probe.

From the absorption spectrum it can be seen that there is only an obvious absorption peak (the first electronic transition of the QDs) located at 506 nm, no any fine structures are observed at shorter wavelength (Fig. S1A). The characteristic of the absorption indicates a rather wide size distribution of the QDs, which results from the effect of Ostward ripening of aqueous synthesis. The band-edge emission of the QDs is 551 nm, and the corresponding full width at half-maximum (FWHM) is about 52 nm (Fig. S1A). It should be pointed out that the large FWHM here is just a very ideal property for obtaining a large emission shift. The mean diameter of the QDs is 2.6 ± 0.4 nm with size distribution $\delta = 15\%$ (Fig. S1B, C), as determined by high resolution transmission electron microscopy (HRTEM) (Fig. S1D). The QD size obtained from HRTEM is in consistent well with that estimated by the first absorption maximum using the empirical formula ($D = (9.8127 \times 10^{-7})\ \lambda^3 - (1.7147 \times 10^{-3})\ \lambda^2 + (1.0064)\ \lambda - 194.84$) reported by Peng group (Yu et al., 2003). In the following experiments, L-cys-capped CdTe QDs with 2.6 ± 0.4 nm in diameter (QDs-1) were chosen for intuitive color change within the given emission shift. The room temperature fluorescence quantum yield (QY) of the crude colloidal solution of QDs-1 was estimated to be 23.28% using Rhodamine 6G as reference. The rather high QY of QDs-1 could provide enough emission intensity to facilitate the observation of the fluorescence quenching at lower pH values.

3.2. pH-dependent emission change of QDs-1

QDs-1 were highly sensitive to the small pH changes under physiological conditions. Fig. 1 showed the emission quenching of the QDs-1 resulting from a decrease of the solution pH value. Significantly, a slight pH change from 7.0 to 6.8 induced a 16.4 nm emission red-shift (from 554.4 nm to 570.8 nm). Meanwhile, TEM images revealed that aggregation of QDs happened as the pH decrease from 7.6 to 6.8 and that finely monodispersed QDs were formed when the pH changed from 6.8 back to 7.6 (Fig. S2).

It was noted that the collective opto-electrical properties of quantum dot materials was influenced by mutual interdot interactions. There are two important interactions, i.e. exciton energy transfer (EET) and electronic coupling (Koole et al., 2006; Wuister et al., 2005). In our case, the electronic coupling between the QDs-1 was weak, since no significant changes in the absorption spectra of QDs-1 were observed (data not shown). Therefore, the emission quenching and red-shift of QDs upon aggregation was most likely attributed to the EET mechanism, where exciton energy of higher bandgap QDs was migrated to smaller bandgap QDs or defect states (Koole et al., 2006).

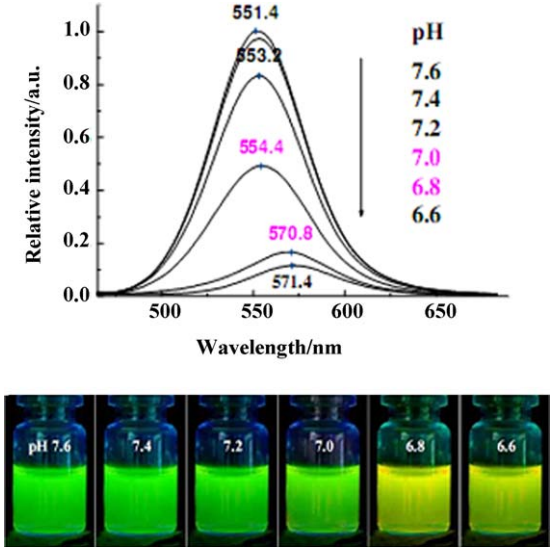

Fig. 1. Fluorescence spectra (top) and emission colors (bottom) of QDs-1 in aqueous solutions of different pH.

The aggregation process of reversibility often results from the non-covalent interactions between particles (Liu et al., 2011). The gel electrophoresis experiment results (Fig. 2) indicated that the QDs migrated quickly towards the positive electrode at pH 7.0, which may be due to the presence of more negative surface charges of the particles. At pH 6.8, which may be the isoelectric point (pH_{ip}) of these particles, the QDs with a lower surface charge stayed very close to their original position. Obviously, electrostatic repulsion between QDs was strong enough for them to be generally isolated at a high pH (>pH_{ip}). Conversely, the electrostatic repulsion was weakened near the pH_{ip}. Thus, the predominantly hydrophobic interactions induced the aggregation of the QDs, which triggered the EET process.

Further evidence for the energy transfer in the QDs-1 clusters was obtained from the time-resolved fluorescence spectroscopy data (Table S1). Fig. S3 showed the fluorescence decay curves for the QDs-1 at two different pH values. A decrease of the decay time was observed as the pH decreased from 7.0 to 6.8, which would originate from the additional decay channels provided by acceptor QDs in clusters. In addition, the fluorescence decay recovered when the pH changed from 6.8 back to 7.0, suggesting that the additional decay channels abated with the disintegration of the QDs clusters due to the electrostatic repulsion between QDs.

The clustered QDs-1 were stable for hours and gave no obvious change in the emission wavelength at a given pH value (Fig. S4). The reversibility of this pH-dependent emission was checked through monitoring the emission change of the solution of QDs-1 during a pH cycle between 7.6 and 6.6. A reasonable reversibility of the emission wavelength was retained for at least one cycle (Fig. S5), although an about 20% intensity loss was observed due to the quenching effect of dissolved oxygen (Fig. S6) (Xia et al., 2007). Here, the reversible emission shifts provided a clear and acute color change, which formed the basis for monitoring alterations in physiological pH even with the naked-eye.

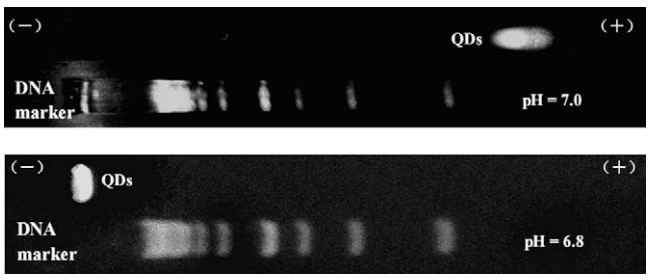

Fig. 2. Gel electrophoresis experimental results.

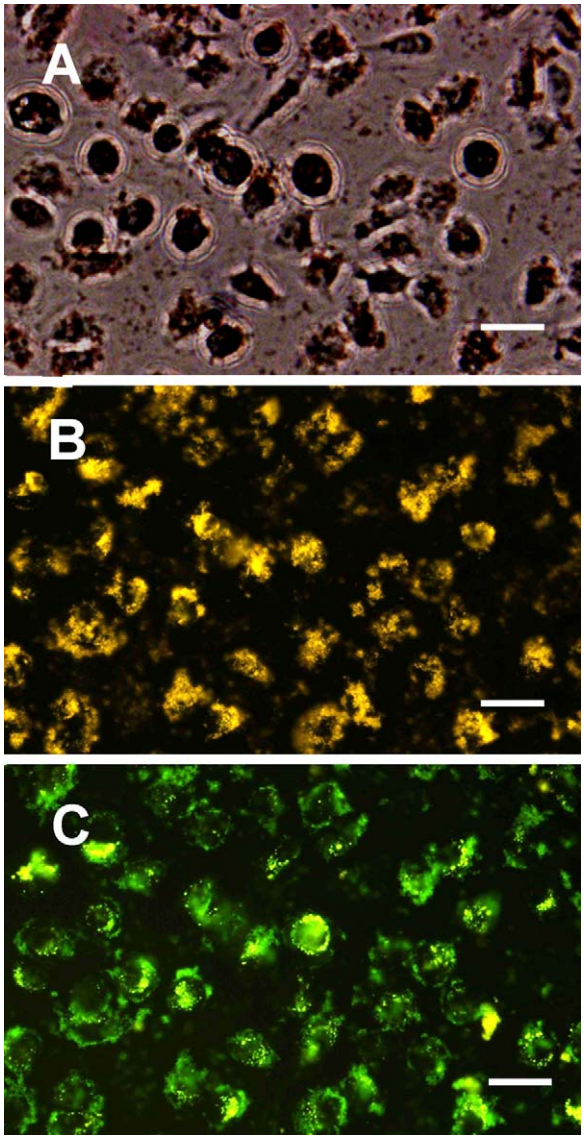

Fig. 3. Bright-field image (A) and fluorescence images (B and C) of the living HepG2 cells incubated with QDs-1 taken after addition of a pH 6.8 buffer (B) and subsequent addition of chloroquine (C) using blue filters. The scale bar = 20 μm.

3.3. *Application of QDs-1 to intracellular pH change indication*

To evaluate the suitability of QDs-1 as an intracellular pH indicator, the effects of pH on the emission color in fixed cells were explored. Considering that QDs-1 was a probe for cytosol at a 6.8–7.4 pH range (Sun et al., 2007; Pal and Parker, 2007), human hepatocellular carcinoma cell lines (HepG2 cells, Manassas, VA) containing QDs-1 were chosen and fixed with formaldehyde; the samples were then mixed with 150 mM phosphate buffer solutions adjusted to specific pH values by adding 0.1 M NaOH or HCl dropwise to obtain the desired pH ±0.1. Fig. S7 showed the fluorescence microscopic images of the dried fixed HepG2 cells taken before and 30 s after adding buffer. The fluorescence of the cells changed from green to yellow after adding pH 6.8 buffer, but remained green after adding pH 7.0 buffer, corresponding to the observations in Fig. 1.

Next, we incorporated QDs-1 into living cells and examined the effects of pH. Bright field transmission image (Fig. 3A) after incubation with QDs-1 showed the clear contour of the living cells. Phosphate buffer solutions (0.1 M, pH 6.8) were first used to decrease the intracellular pH, and led to a yellow emission (Fig. 3B). Subsequently, a solution of chloroquine (0.1 mM) was used. Chloroquine is a weakly basic amine that tends to concentrate in the lysosomes of living cells and causes an intravesicular pH increase (Caplan et al., 1987; Liu et al., 2007). After 10 min of chloroquine treatment, the fluorescence changed to green due to the pH increase (Fig. 3C). These results demonstrated that L-cys-coated CdTe QDs could be applied to quickly indicate the slight variation of intracellular physiological pH.

From Fig. 3 it also can be confirmed that the cells are viable under the experimental conditions. The clear contour of the cells showed in Fig. 3A indicated that most of the cells are adherent cells (Jones and Grainger, 2009). Meanwhile, Fig. 3B and C showed that the emission color mainly located in the edge of the nucleus, where the lysosomes were concentrated (Zhou et al., 2010). If the cells were dead, lysosomes would have been broken (Kirkegaard and Jäättelä, 2009), and the specific emission distribution would be lost. Clearly, the cytotoxicity of QDs-1 was not obvious. The survival time of living cells is at least 6 h after incubation with QDs-1 according to our observation, which is important for monitoring pH change of some cellular processes.

Largely, the toxicity of QDs in biological systems is not dependent on the QDs particle itself but on the amount of free Cd^{2+} in solution of QDs (Cho et al., 2007; Hoshino et al., 2004). For designing less-toxic QDs, it is important to select hydrophilic biomolecules to dissolve QDs in water (Hoshino et al., 2004). In our case, the QDs-1 was well modified by L-cys, a hydrophilic biomolecule, and was purified carefully before the imaging test. Furthermore, the imaging was performed in the vicinity of pH 7.0, in which QDs-1 could be stabilized by means of the possible secondary coordination (Gao et al., 1998) between the carboxyl O atom from L-cys and the Cd atom at the CdTe particle surface. All of these may be favorable for decreasing the leakage of Cd^{2+} and maintain the activity of the cells.

4. Conclusions

Here we have demonstrated a simple method for tracking intracellular physiological pH changes, based on an efficient EET process in the nominally single-sized colloid solution samples of the L-cysteine-capped CdTe QDs with intrinsically broadened size distributions. With the rational design of the QD surface chemistry, it is promising to develop a general emission color change-based sensing strategy for other analytes or processes.

Acknowledgements

This work is financially supported by NSFC project (Nos. 20875003 and 20905002).

Appendix A. Supplementary data

Supplementary data associated with this article can be found, in the online version, at doi:10.1016/j.bios.2011.09.005.

References

Alivisatos, A.P., 1996. Science 271, 933–937.
Aronson, P.S., Boron, W.R., 1986. Na^+-H^+ Exchange, Intracellular pH, and Cell Function. Academic Press, New York.
Caplan, M.J., Stow, J.L., Newman, A.P., Madri, J., Anderson, H.C., Farquhar, M.G., Palade, G.E., Jamieson, J.D., 1987. Nature 329, 632–635.
Cho, S.J., Maysinger, D., Jain, M., Röder, B., Hackbarth, S., Winnik, F.M., 2007. Langmuir 23, 1974–1980.
Gao, M., Kirstein, S., Möhwald, H., Rogach, A.L., Kornowski, A., Eychmüller, A., Weller, H., 1998. J. Phys. Chem. B 102, 8360–8363.
Helmlinger, G., Yuan, F., Dellian, M., Jain, R.K., 1997. Nat. Med. 3, 177–182.
Hoshino, A., Fujioka, K., Oku, T., Suga, M., Sasaki, Y.F., Ohta, T., Yasuhara, M., Suzuki, K., Yamamoto, K., 2004. Nano Lett. 4 (11), 2163–2169.
Jones, C.F., Grainger, D.W., 2009. Adv. Drug Deliv. Rev. 61 (6), 438–456.
Jones, J.M., Lorton, S.P., Bavister, B.D., 1995. Cytometry 19, 235–242.
Jr, P.A., Tyson, D.S., Jursíková, K., Castellano, F.N., 2002. J. Am. Chem. Soc. 124, 6232–6233.
Kirkegaard, T., Jäättelä, M., 2009. Biochim. Biophys. Acta 1793, 746–754.
Koole, R., Liljeroth, P., Donegá, C.M., Vanmaekelbergh, D., Meijerink, A., 2006. J. Am. Chem. Soc. 128, 10436–10441.
Liu, J.B., Yang, X.H., Wang, K.M., Yang, R.H., Ji, H.N., Yang, L.Y., Wu, C.L., 2011. Chem. Commun. 47, 935–937.
Liu, Y.S., Sun, Y.H., Vernier, P.T., Liang, C.H., Chong, S.Y.C., Gundersen, M.A., 2007. J. Phys. Chem. C 111, 2872–2878.
Martin, G.R., Jain, R.K., 1994. Cancer Res. 54, 5670–5674.
Matsuyama, S., Llopis, J., Deveraux, Q.L., Tsien, R.Y., Reed, J.C., 2000. Nat. Cell Biol. 2, 318–325.
Moolenaar, W.H., Tertoolen, L.G.J., Delaat, S.W., 1984. Nature 312, 371–374.
Moon, J., Choi, K., Kim, B., Yoon, K., Seong, T., Woo, K., 2009. J. Phys. Chem. C 113, 7114–7119.
Murphy, C.J., 2002. Anal. Chem. 74, 520A–526A.
Narayanan, S.S., Pal, S.K., 2006. J. Phys. Chem. B 110, 24403–24409.
Ohmichi, T., Kawamoto, Y., Wu, P., Miyoshi, D., Karimata, H., Sugimoto, N., 2005. Biochemistry 44 (19), 7125–7130.
Pal, R., Parker, D., 2007. Chem. Commun., 474–476.
Schindler, M., Grabski, S., Hoff, E., Simon, S.M., 1996. Biochemistry 35 (9), 2811–2817.
Sun, K.M., McLaughlin, C.K., Lantero, D.R., Manderville, R.A., 2007. J. Am. Chem. Soc. 129, 1894–1895.
Tang, B., Liu, X., Xu, K.H., Huang, H., Yang, G.W., An, L.G., 2007. Chem. Commun., 3726–3728.
Wuister, S.F., Koole, R., de Mello Donegá, C., Meijerink, A., 2005. J. Phys. Chem. B 109, 5504–5508.
Xia, Y.S., Zhang, T.L., Diao, X.L., Zhu, C.Q., 2007. Chem. Lett. 36 (2), 242–243.
Xia, Y.S., Zhu, C.Q., 2008. Analyst 133, 928–932.
Yu, W.W., Qu, L., Guo, W., Peng, X., 2003. Chem. Mater. 15, 2854–2860.
Zhou, F.F., Xing, D., Wu, B.Y., Wu, S.N., Ou, Z.M., Chen, W.R., 2010. Nano Lett. 10 (5), 1677–1681.